

# FUNDAMENTALS OF STEEL MICROALLIGATION

C. Mapelli, R. F. Riva

*The micro-alligation of steels has become a usual practice during the last decades for the positive results which can be reached in terms of yield strength, toughness and plastic formability also through a modulation of the properties which can be obtained only by the choice of a correct cooling rate and the control of the final forming temperature of the steels. The micro-alligation can grant significant advantages in terms of the mechanical properties and in terms of economic savings related to avoiding the alligation of expensive chemical elements and the elimination of long heat treatment.*

**KEYWORDS:** steel, microalligation, mechanical properties

## INTRODUCTION

The final satisfactory performances of the micro-alloyed steels involved the correct technical management of the whole production process<sup>1)</sup>:

- addition of the correct quantity and type of micro-alloying elements;
- application of suitable operative parameters of solidification process (continuous casting machine and ingot solidification);
- choice of the thermal range in which the plastic forming procedure is performed, the final temperature of the deformation process and the cooling rate to be applied.

All these aspects have to be correctly taken into account in order to exploit the micro-alligation avoiding dangerous drawbacks. At the present state of the art the main exploited elements for the micro-alligation are<sup>1,2,3,4,5,6)</sup>:

- titanium
- niobium
- vanadium
- aluminium (because the precipitation of AlN performed primarily reduces N content in liquid steel but refines also the grains)
- boron

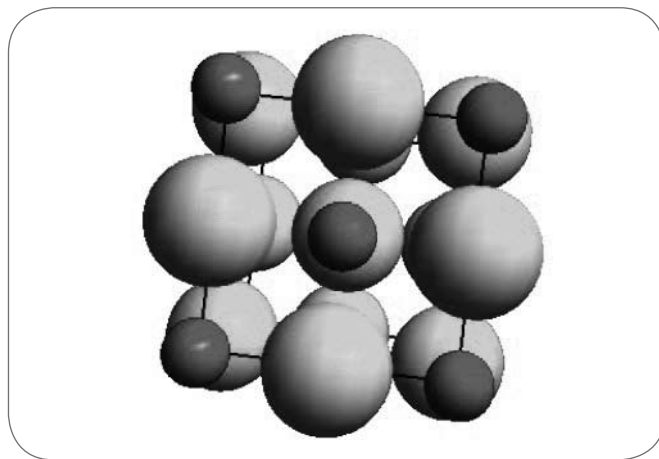
but the mechanism through which they performed their actions are different and the activation of this mechanisms takes place in different temperature ranges. Among the main strengthening mechanisms can be recognized:

- interaction between precipitated particles and the dislocations, resulting in the hindering of dislocation movement;
  - refining of the ferrite grains;
  - induction of microstructure which are not in thermodynamic equilibrium, i.e. bainite for the particular case of boron addition.
- Thus, in this presentation around the fundamentals of microalligation the aspects related to:
- the strengthening mechanisms;

- thermodynamics of micro-alligation;
  - the damaging mechanism inducing the hot shortness and promoted by the presence of micro-alloying elements;
  - the control of the microstructure during the thermo-mechanical cycles
- will be synthetically taken into account.

## THE STRENGTHENING MECHANISMS

Titanium, niobium and vanadium perform the strengthening action by the precipitation of ceramic carbide or nitride compounds featured by nano-scale size<sup>1)</sup>. All these compounds are characterized by a centred cubic cell of NaCl type (Fig. 1) and they interact with dislocations, making their movement ex-

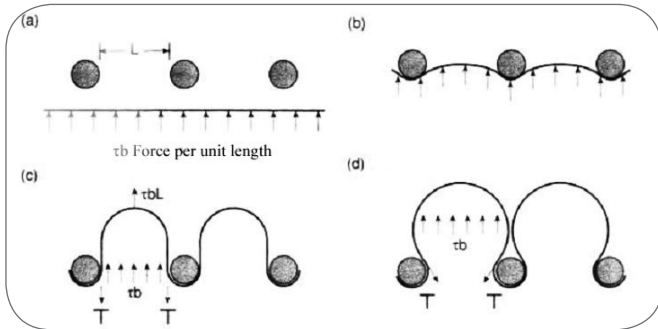


▲  
Fig. 1  
**Representation of a cell of NaCl type. The position of the small spheres shown in the cells within carbide or nitride formed by the micro-alloying elements are occupied by C or N.**

Rappresentazione di una cella elementare del tipo NaCl, dove le sfere piccole rappresentano gli spazi occupati dagli elementi interstiziali che, nel caso dei composti formati all'interno degli acciai microlegati, sono N e C.

Carlo Mapelli, Riccardo F. Riva

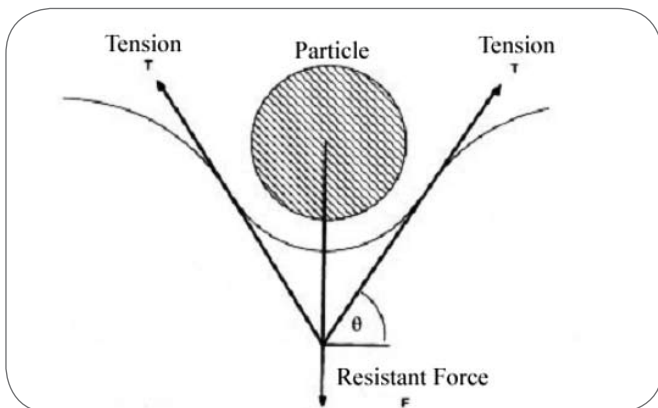
Dipartimento di Meccanica del Politecnico di Milano  
Via La Masa 34, 20156 MILANO (ITALY)



▲  
Fig. 2

**Steps through which the dislocation can push through the precipitate arrays embedded in the metal matrix. (a) Dislocation is approaching the ceramic particles array, (b) sub-critical situation of deformation, (c) critical situation for the deformation of the dislocation line, (d) deformation corresponding to the condition of dislocation leakage from the arrays of the ceramic precipitated particles.**

*Stadi del processo di interazione tra una dislocazione e le particelle ceramiche formate dai microleganti. (a) La dislocazione si avvicina alla schiera delle particelle ceramiche, (b) situazione di deformazione sub-critica, (c) situazione critica per la deformazione della linea di dislocazione (d) deformazione corrispondente alla condizione di fuga della dislocazione dalla schiera delle particelle ceramiche precipitate.*



▲  
Fig. 3

**Force balance between the resistance offered by the particles against the dislocation motion and the tension developed on the dislocation line.**

*Bilancio delle forze tra la resistenza al movimento offerta da un precipitato e la tensione indotta sulla dislocazione.*

remely difficult. Only the aluminium nitride is featured by an hexagonal compact cell which does not allow its combination with the non-metallic compounds formed by the other elements. This process implies an increase of the yield strength featuring the steel<sup>7,8,9,10</sup>.

One of the most valuable model proposed by Orowan<sup>1,2</sup> when the dislocations sliding within the metal matrix encounter a nano-precipitate array, a mechanical equilibrium between the stressed dislocation line and the repulsive force developed by the non-metallic particle is reached. The shape assumed by the dislocation line is ruled by the principle of energy minimization (Fig. 2, Fig. 3).

The trapping forces developed by the particles depend on the average spacing between the precipitates composing the arrays. If a bi-dimensional model is assumed for the particle distribution the yield strength can be suggested through the relation:

$$\sigma_y = \sigma_m + 6Gb(3f/2\pi)^{0,5} / X \quad (1)$$

where  $\sigma_m$  represents the yield strength in absence of precipitation,  $G$  is the tangential elasticity module ( $G=E/2(1+\nu)$ ),  $b$  is the lattice characteristic parameter,  $f$  is the volume fraction of the precipitates and  $X$  represents their average diameter. This relation tends to overestimate the increase of the yield strength so it can be regarded as an upper boundary limit to the strengthening mechanism. Other more modern approaches performed on the basis of 3D finite element simulation allow a more general treatment of this aspect. Ashby<sup>2</sup> proposed a relation which takes into account also the spacing between the precipitate surfaces as a significant parameter and not the distance between the centres of the particles. This statement implied a modification of the former relations. This has permitted to obtain more reliable values consistent with the experimental measurements:

$$\Delta\sigma_y (MPa) = (10,8 \cdot f^{0,5} / X) [\ln (X/6,125 \cdot 10^{-4})] \quad (2)$$

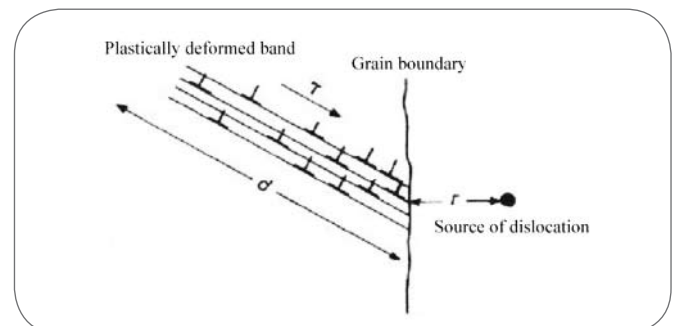
Thus, the most favourable condition is represented by:

- precipitation of a high volume fraction of ceramic particles;
- very fine nano-particles (5-40nm);
- and the two previous conditions imply that a favourable situation is associated with the very narrow spacing between two successive particles constituting the arrays of the nano-precipitates.

Through TEM observations has been stated that the size of the nano-precipitates have not to exceed the value of 35-40nm, otherwise their effect can be detrimental on the toughness, because their accumulation on the grain boundaries can promote the detachment among the grain surface which is further weakened by the presence of the ceramic particles of large size.

The precipitates can take part also to the refining process of the grain size and for this second strengthening modality also the AlN can play a very significant role. This strengthening mechanism can improve also the toughness because it implies (Fig. 4):

- the locking and the stacking up of the dislocation on the grain boundaries which increase the yield strength;
- the induction of new dislocations in the grains which are



▲  
Fig. 4

**Mechanism of pile up of dislocations on a grain boundary and arising of a new one in an adjacent grain. Meccanismo di impilamento delle dislocazioni su un bordo grano e punto di insorgenza di una nuova dislocazione all'interno del grano adiacente.**

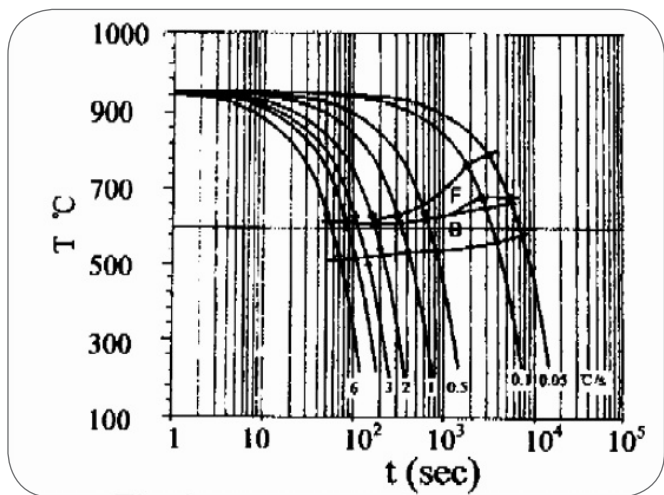


**Fig. 5** Anisotherm cooling diagram for a 12ppm boron alloyed steel. It is evident the significant width of the bainite formation field<sup>6)</sup>.

Curva anisoterma di un acciaio alligato con 12ppm di boro. E' evidente il significativo allargamento del campo di formazione della bainite<sup>6)</sup>.

subjected to the pressure of the dislocation stacking up on the boundaries of the adjacent grains. The formation of new dislocations is associated to an energy expense that increases the attitude of steel in the energy dissipation and consequently to a ductile behaviour.

The grain refinement mechanism cannot be exploited in casting products, because the refining effect is associated to the microstructural transformations promoted by the energy supplied to the steel and stored by it during the transformation process. Actually, the precipitates perform a pinning action on:

- the dislocations introduced by the deformation, which reorganize themselves in dislocation walls during the recovery process;
- the boundaries of the recrystallized grains.

It is worth noting that the step involving the plastic deformation process is needed in order to realize the desired refining through the exposed mechanisms.

The delaying in the recovery kinetics caused by interactions with precipitates produces a delaying also in the activation of the recrystallization process which implies a decrease of the time which can be spent for the successive growth of the grains. This statement is conformed also by the increase of about 25-30% in the activation energy of recrystallization revealed in the steels micro-alloyed by titanium<sup>3)</sup>.

A strong refining action is performed also by vanadium, because in the concentrations generally present in the chemical composition of the steel its ceramic compounds precipitate near the austenite-ferrite transition temperature inducing an efficient refinement of the ferrite grains.

The strengthening mechanism produced by the grain refining is cumulated with the dislocation locking performed by the ceramic particles and these two effects can be summed in a unique expression taking into account the effect of grain refining described by the Hall-Petch relation<sup>4)</sup>:

$$\sigma_y = \sigma_i + \sum k_i \cdot c_i + k_y \cdot d^{0.5} + (10,8 \cdot f^{0.5} / X) [\ln (X/6,125 \cdot 10^{-4})] \quad (3)$$

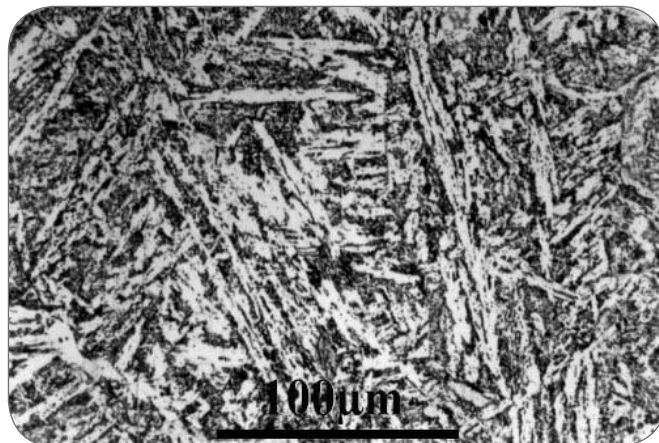


**Fig. 6** Example of bainite structure developed in a steel alloyed by 25ppm of B<sup>6)</sup>.  
Esempio di bainite formata all'interno di un acciaio alligato con 25ppm di B<sup>6)</sup>.

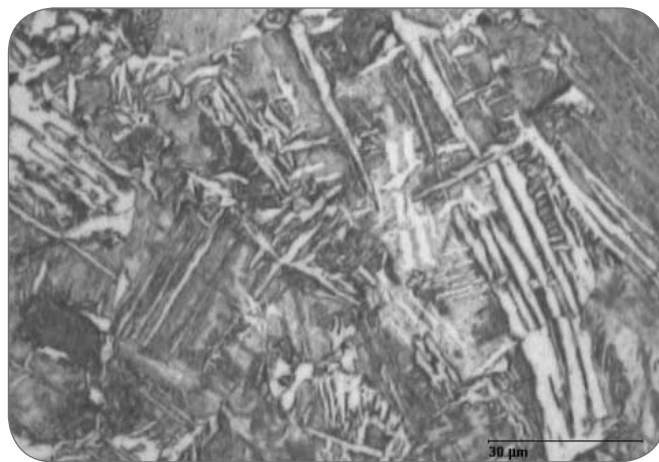


**Fig. 7** Example of acicular ferrite in a steel alloyed by 15ppm B.  
Esempio di ferrite aciculare in un acciaio alligato con 15ppm di boro.

In steels micro-alloyed by 0.05%V the increase in  $\Delta\sigma_y$  can reach 150MPa.

The strengthening mechanism produced by the boron introduced in the steel is inspired to a completely different concept related to the formation of metallurgical structure which are not thermodynamically stable, i.e. bainite.

The boron tends to concentrate on the grain austenite boundaries delaying the ferrite formation, because it slows the nucleation of this phase. This causes a shift of the ferrite transformation in a lower temperature range, but this decrease of the thermal range causes a not complete arrangement of the transformed phases inducing the formation of acicular ferrite or even of bainitic structure. It is interesting to note how the boron addition extends the bainite formation field in the anisotherm cooling diagram (Fig. 5)<sup>6,7,8)</sup>. The formation of acicular ferrite in steels alloyed by boron can be revealed also in the core of continuously cast billets which do not undergo drastic cooling (Fig. 6, Fig. 7).

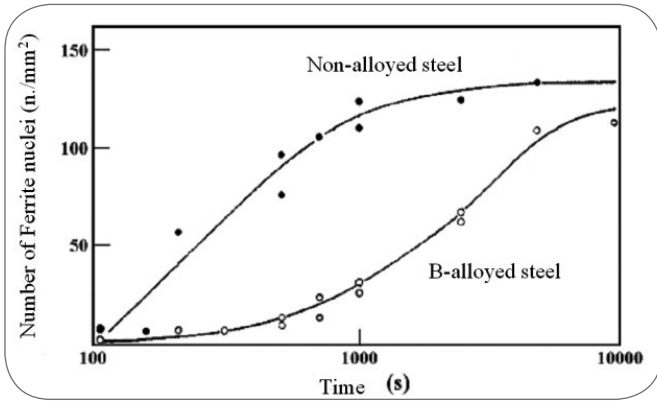


**Fig. 8** Example of the decreasing in the nucleation of ferrite promoted by the boron addition. Esempio della diminuzione nel tasso di nucleazione della ferrite a seguito dell'aggiunta di boro in lega.

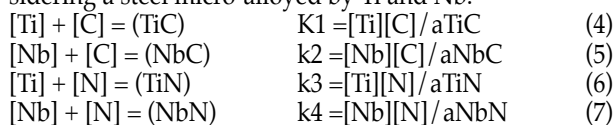
It is important to note that the only boron content which can contribute to the formation of distorted structural constituents is the one maintained in solution within the metal matrix and not the quantity combined with other elements, i.e. N, because only the content of boron in solution can segregate to grain boundaries in order to perform the delayed nucleation of ferrite from austenite (Fig. 8)<sup>9,10</sup>. A practical and usual evaluation of the boron efficiency can be realized by the realization of the Jominy test.

**THEMODYNAMICS AND KINETICS OF MICRO-ALLIGATION**

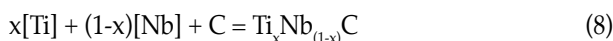
The precipitation of the ceramic precipitates is ruled by the solubility products which can be computed on the basis of thermodynamic data contained in literature<sup>9</sup>. As a first approximation the activity coefficient of the microalloying elements can not be included in the thermodynamic computation exploiting the extremely low concentration of the microalloying elements<sup>1,4,11,12,13</sup>:

- Ti and Nb 0.01-0.04%;
- V 0.01-0.2%;
- Al 0.02-0.08%.

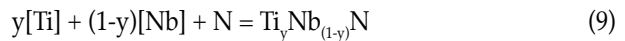
From a computational point of view the evaluation of the amount of the precipitated ceramic phases is complicated by the mutual solubility of carbides and nitrides formed by Ti, Nb and V due to the very similar lattice parameters featuring their crystal cells. In this case the solubility product cannot provide a significant information, because the activity of the formed compounds cannot be set at 1, but they have to assume the value imposed by the mutual solubility of those compounds in the formed precipitates. This fact makes the computation problem more difficult to be solved. This can be evaluated considering a steel micro-alloyed by Ti and Nb:



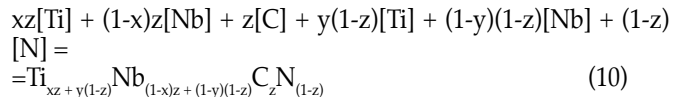
where ai represents the activity of -ism generic component. For the formation of complex carbide it is needed to consider:



while for the formation of a complex nitride the relation to be taken into account is:



Where x and y are the atom fractions of Ti in the considered compounds. Finally, the formation of a complex carbo-nitride takes the form:



where z is the fraction of the interstitial carbon atom entering in the complex carbo-nitride. Thus, on the basis of the statistical possibility of combination among the different species the activities of the different compounds present in the precipitates can be described as:

$$a_{TiC} = xz \quad a_{NbC} = (1-x)z \quad (11)$$

$$a_{TiN} = y(1-z) \quad a_{NbN} = (1-y)(1-z) \quad (12)$$

Through the substitution of this relation in the mass balance and in the equilibrium solubility relations it is possible to reach a reliable information about the amount and type of the formed complex precipitates. This thermodynamic information has to be coupled with the kinetic ones which rule the size of the precipitated compounds. The kinetic control is determined by the two classic mechanisms of nucleation and growth of the phases<sup>1,12,13,14,15,16</sup>(Fig. 9, Fig. 10): The evaluation of the form assumed by the precipitation curve clearly indicates that the process is ruled by a nucleation

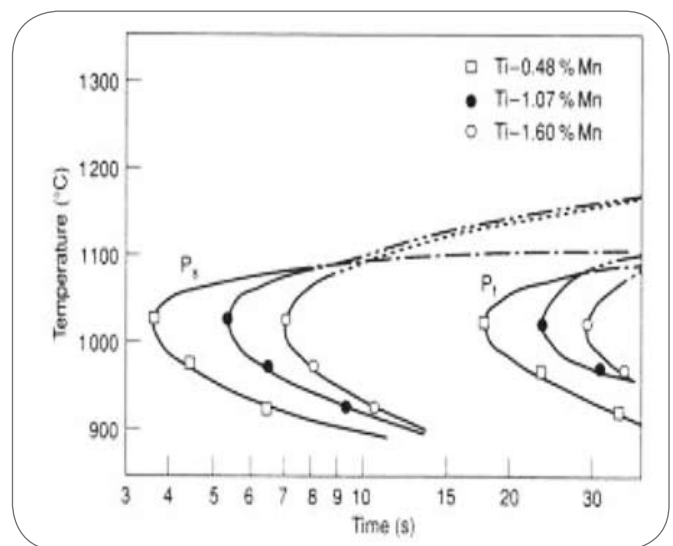


**Fig. 9** Precipitation curve of TiC in 0.01% Ti micro-alloyed steel alloyed by different Mn content<sup>15</sup> and hot rolled at 0.028s-1(after Gladman). Curva di precipitazione del TiC in un acciaio micro-alligato con 0.01% di Ti laminato con un tasso di deformazione pari a 0.028s-1, in funzione di differenti tenori di Mn (Gladman).

and growth process. The higher temperature range favours the growth of few precipitates which can nucleate in that high temperature range, while the lower temperature ranges promote an intense nucleation of the ceramic particles but a weak growth process due to a higher undercooling and to the simultaneous inhibition of the diffusive phenomenon which rules the growth process. On the basis of the statement exposed in the section dedicated to the strengthening mechanism the condition featured by a lower temperature range is the most favourable in order to exploit the advantages of micro-alloying, because it avoids the formation of coarse precipitates (Fig. 11). Moreover, the slowing imposed to the diffusion phenomena maintains a fraction of the micro-alloyed elements in solution through a fast cooling. This allows also the occur-

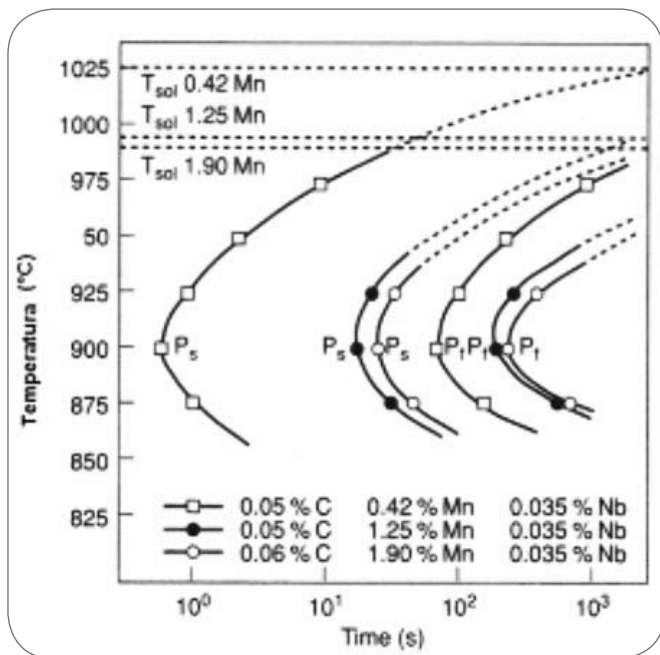


**Fig. 10**  
**Precipitation curve of NbC in 0.035% Nb microalloyed steel alloyed by different Mn content (16) after hot rolling featured by a 50% reduction (after Gladman).**

Curva di precipitazione del NbC in funzione del contenuto di Mn in un acciaio microalligato con 0.035% di Nb, a seguito di una laminazione con una riduzione di spessore del 50% (Gladman).

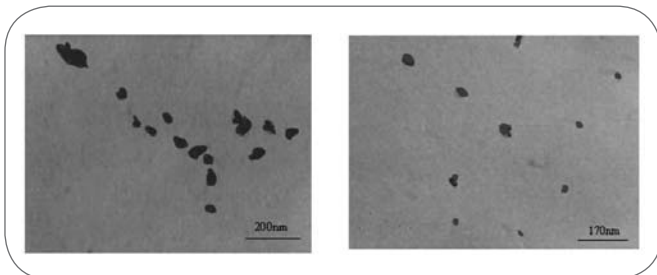


**Fig. 11**  
**Example of several precipitates formed by the micro-alloyed elements and observed by TEM.**  
 Esempio di diversi precipitati osservati mediante TEM in acciai microalligati.

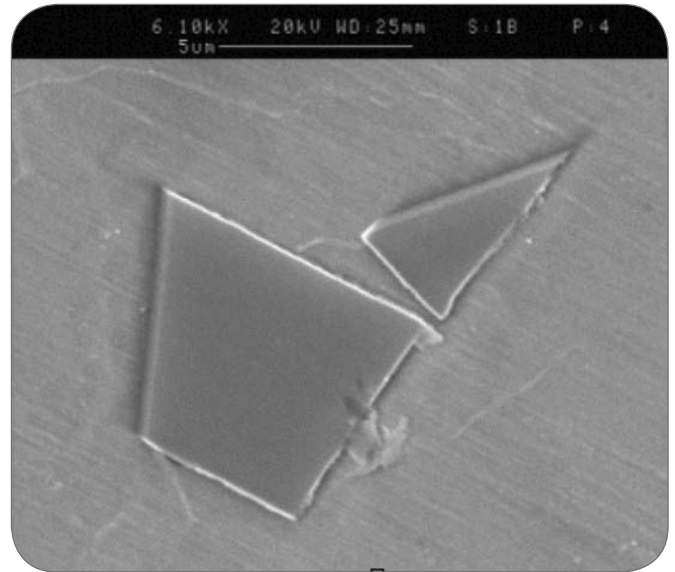


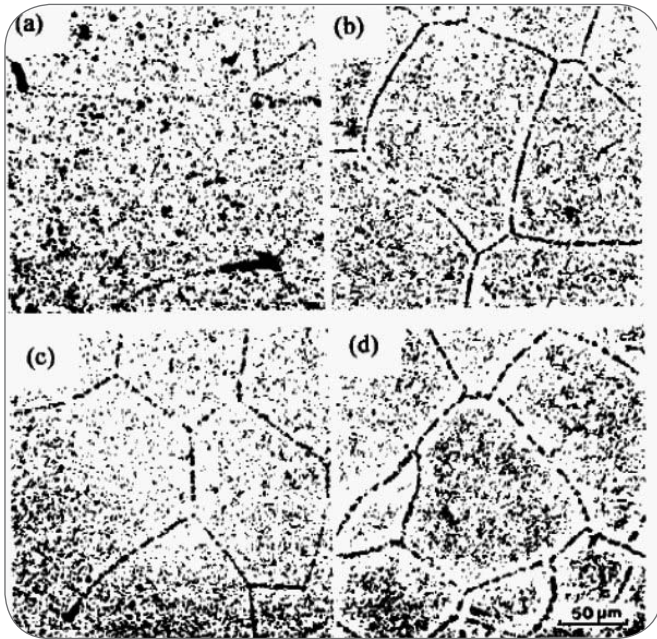
**Fig. 12**  
**Example of large-size TiN revealed in a Ti microalloyed steel (by R. Venturini).**  
 Esempio di TiN di grandi dimensioni in un acciaio microalligato con Ti. (R. Venturini).

rence of strain aging phenomena within the steels which can be exploited even in the bake-hardening treatment<sup>17)</sup> which can produce an increase between 13-18% of the yield strength of the micro-alloyed steel, but also the sudden decrease of ductility properties.

The precipitation of coarse non-metallic compounds due to a not correct addition of the alloying elements can be extremely dangerous especially in the steels microalloyed by Ti, when the possible precipitation of this compound even in the liquid phase can produce dangerous and detrimental non-metallic compounds. The addition of Ti is often used in order to sequester N which can combine with boron (forming BN that causes the increase of the steel brittleness) or with Al inducing problem of hot shortness in the steel. On the other hand, this application has to be strictly controlled in order to avoid the formation of the non-metallic edged inclusions of TiN which can be the nucleating element of a fatigue fracture (Fig. 12). Moreover, the use of Ti as micro-alloying elements has to be carefully performed by the steelmakers, because the Ti added in one heat can pollute the chemical composition of the other heats treated in the same ladle.

For the boron micro-alloyed steel the thermodynamic interest has to be focused on avoiding the formation of BN during the ladle treatment and the continuous casting. The protection of B is usually performed by the addition of Ti and Al. The protection of boron has to be granted in order to permit the accumulation of B in solution at the grain boundaries of austenite. The heat treatment applied to boron micro-alloyed steel has to be performed from a temperature range which allows the accumulation of boron in solution on the grain boundaries and this has been clearly shown by Wang et He (Fig. 13).

Only a complete austenitization and a temperature which permits the rapid diffusion of boron towards the grain boundaries can permit to exploit its delaying effect on the ferrite nucleation. Thus, the highest maintaining temperature ranges appear the most favourable one from this point of view.



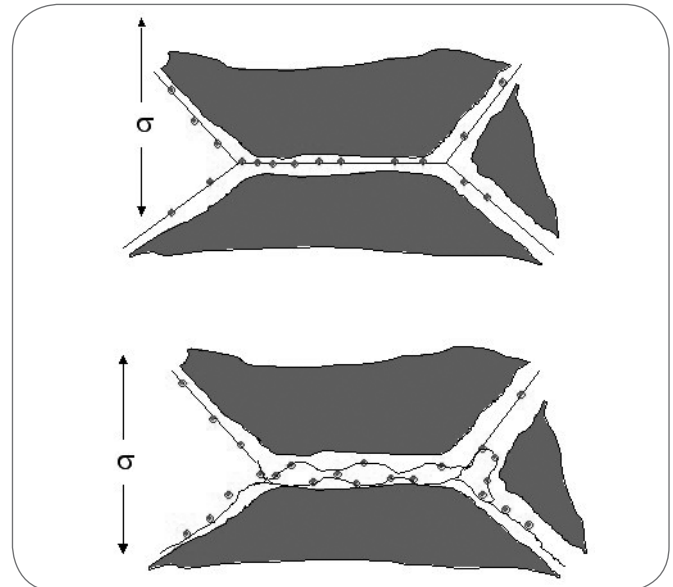
▲  
Fig. 13

**Different distributions of boron as function of the heating temperature (a)800°C (b)900°C (c) 1000°C (d)1150°C (after Wang and He)<sup>6]</sup>.**  
*Differente distribuzione del boro sui bordi grano austenitici in funzione delle temperature di riscaldamento precedenti il raffreddamento (a)800°C (b)900°C (c) 1000°C (d)1150°C (Wang and He)<sup>6]</sup>.*

## DRAWBACKS AND INDUCTION OF HOT SHORTNESS AND BRITTLENESS

The hot shortness represents a dangerous problem during the continuous casting operation and during the hot forming operation. The hot shortness temperature range is between 1050°C and 700°C. The observed drop in the ductility is increased with increasing the content of Ti, V, Al, Nb because these chemical elements have the property to produce the precipitation of particles on the grain boundaries which represent the weak region of a micro-structure. The hard cooling and the soft cooling strategies followed during the continuous casting of the micro-alloyed steels has to be performed in order to avoid the production of cracks due to the rising of hot shortness mechanisms. The failure mechanisms produced by the precipitates on the grain boundaries in the indicated thermal range can be summered in three main failure processes. The first two mechanisms are analogous and lead to intergranular fracture on the interface perpendicular to the direction of stress application (Fig. 14). In the first variant of the mechanism the precipitation of ceramic compounds decreases the micro-alloying content on the adjacent steel regions weakening these volumes of the materials which can fail under the applied stress. In the second variant the precipitated pro-eutectoid soft ferrite can be damaged by ceramic compounds under the stress action producing the complete failure of the interface. A third mechanism implies the failure in direction parallel to the stress application one according to a mechanism which is analogous to the failure produced by the creep process (Fig. 15).

In the boron steels the most dangerous drawbacks can be



▲  
Fig. 14

**Scheme of the failure mechanism on a grain interface perpendicular to stress direction in presence of the precipitation on grain boundaries.**  
*Schema del meccanismo di danneggiamento sull'interfaccia di bordo grano interessata dalla precipitazione di particelle non metalliche e disposta perpendicolarmente rispetto alla direzione di applicazione dello sforzo.*

produced by the precipitation of:

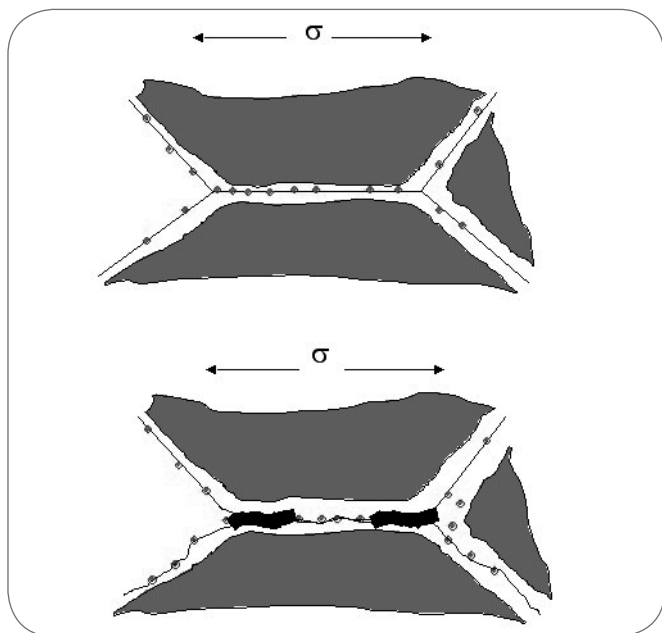
- boron nitride BN;
- intermetallic iron boride Fe<sub>2</sub>B.

These two phases can cause a strong brittleness on the final products. The BN can be avoid by a correct denitruration of the steel liquid bath, while the intermetallic phases can precipitate for a non correct maintaining temperature before the application of the thermal treatment or during the plastic deformation. The DSC-DTA experiments have shown that the precipitation of Fe<sub>2</sub>B is strongly promoted for heating temperature over 1200°C and this phenomenon has to be avoided (Fig. 16).

The precipitation of Fe<sub>2</sub>B in the austenitic field produces an effect not completely understandable on the basis of the traditional optical microscope observations. Actually, in the case of Fe<sub>2</sub>B precipitation, the intermetallic phase precipitating on the grain boundaries contributes in pinning the austenite grains and in refining them, producing finest final ferrite grains which do not correspond with an expected increase of the toughness but with a dangerous decrease of this property. This is due to the weakness induced by intergranular precipitation of the boride which completely balances the refining realized in the microstructure.

## THE EXPLOITATION OF NANO-PRECIPITATION DURING THE THERMOMECHANICAL PROCESSING OF STEELS

The aim of controlled forming process of microalloyed steels is to obtain required properties by controlling the final microstructure without applying a specific heat treatment. The final microstructure and mechanical properties

▲  
Fig. 15

**Scheme of the failure of the grain interface in direction parallel to the stress one.**

*Schema del meccanismo di danneggiamento sull'interfaccia di bordo grano interessata dalla precipitazione di particelle non metalliche e disposta parallelamente rispetto alla direzione di applicazione dello sforzo.*

depend strongly on the chemical composition, on the controlled rolling parameters and on the cooling conditions of the plate<sup>19</sup>.

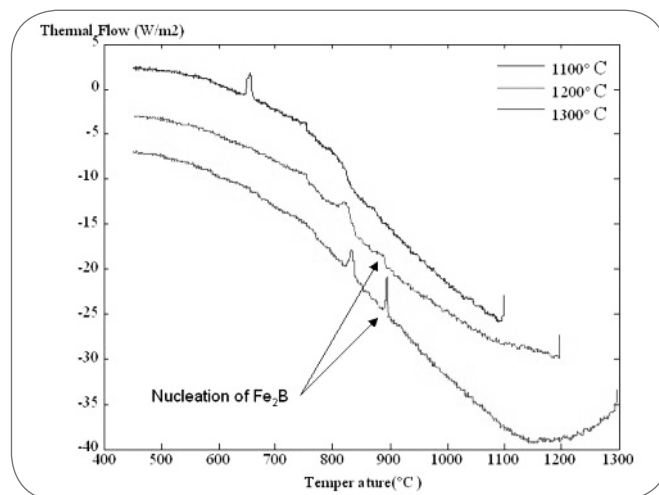
Thermomechanical controlled rolling of microalloyed steel plates is then carried out to provide grain refinement and thus obtain higher strength and toughness properties. Microalloying elements (such as Nb and V) and their carbonitride precipitates limit austenite grain growth at reheating temperature and retard austenite recrystallisation during controlled rolling<sup>20,21,22</sup>.

The consequence of the thermomechanical controlled rolling is that the resulting microstructure can be a mixture of groups of very fine ferrite grains, that nucleated in the deformed austenite in an intra-granular manner, and recovered (and even partially recrystallized) ferrite grains<sup>23</sup>.

The presence of the nano-precipitates and their action on the dislocations makes slower the reorganization of the dislocations to form the subgrains which precede the recrystallization. Moreover, the formation of the nano-precipitates composed by Nb(C,N) within the austenite can nearly stop the growing process of the first recrystallized structures due to the interference realized by the nano-precipitates along the boundary grains featured by high relative angles of misorientation<sup>24</sup>. The V performs its role in a lower thermal range which characterizes the transition from the austenite to the ferrite, because this is the same temperature range which promotes the precipitation of VC which interferes with the ferrite grain boundaries. The presence of the precipitates at the grain boundaries make the grain growth slower, avoiding the grains featured by the most unfavourable textures to consume the grains in which the former austenitic textures have indu-

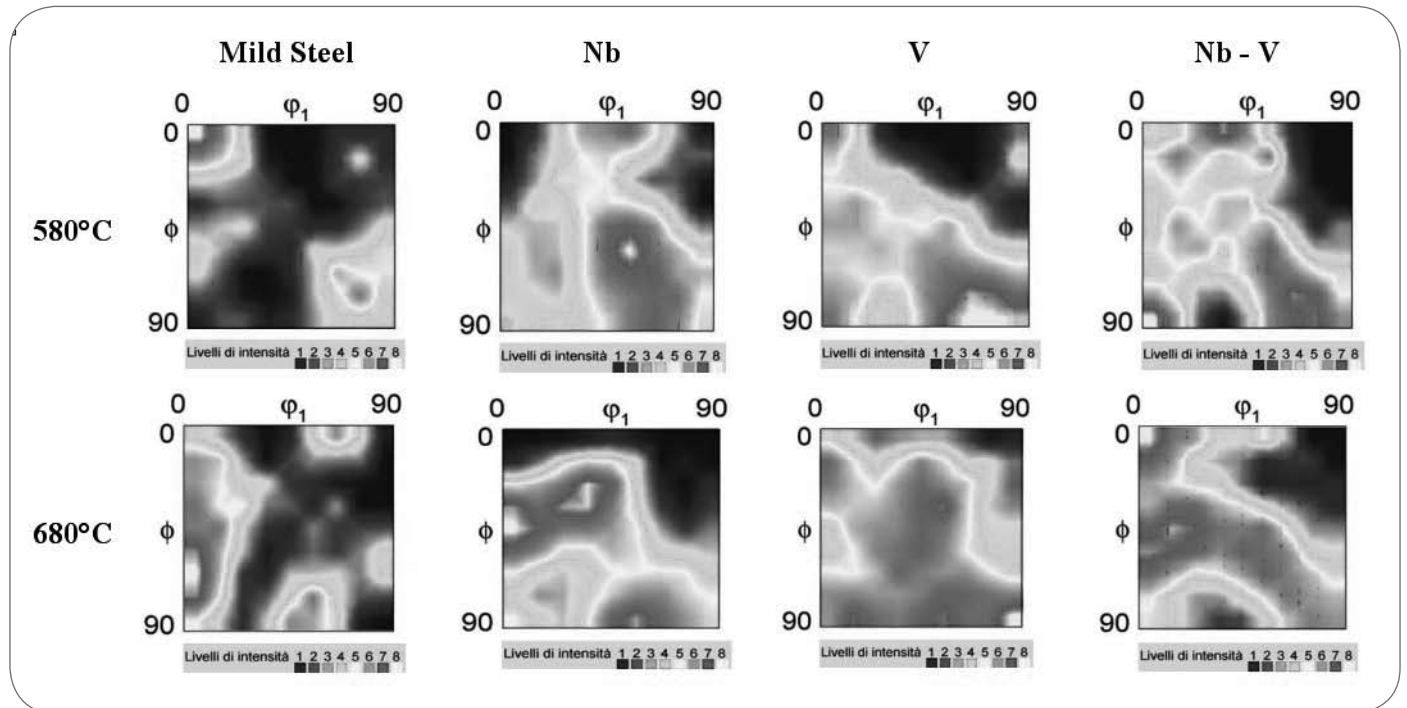
ced the most suitable orientations to assure a good combination among the plastic formability, the strength and the toughness. This consumption takes place through the grain growth phenomenon. The contemporary alloying by Nb and V is one of the most interesting operations to be applied in the most modern productive processes of steel sheets which are featured by the thin casting process and by the in line strip rolling, because these microalloying metal elements develop their actions in a different thermal range<sup>25,26</sup>. The only factor of influence which can be effectively managed by the operators is represented by the control of the final temperatures of rolling steps and the ones characterizing coiling temperatures of the rolled strips. Through the control of these process parameters of recrystallization, the phase transformation and the related development of the crystallographic textures can be correctly managed as a function of the type and of the content of the alloying elements. Nowadays, although the formerly general indications contained in the literature, reliable scientific and quantitative relations describing the mutual interactions between the thermo-mechanical cycle and the formation of the crystallographic textures are not available.

The presence of the nano-precipitates hinders the movement of the dislocations increasing the yield strength and the hindering rate of the steel, but it usually implies a decreasing of the ductility and of the plastic formability which characterizes the traditional mild steels suitable for the forging process<sup>27,28,29,30</sup>. The studies performed at a macro-textures level imply the consideration of a large amount of

▲  
Fig. 16

**DSC-DTA curves measured for 19ppm boron alloyed steel showing the peak indicating the precipitation of the iron boride at 900°C only for the steels reheated over 1100°C. The peak indicating such a formation is particularly evident in the steel reheated at 1300°C.**

*Curve DSC-DTA misurate in un acciaio alligato con 19ppm di boro, ove si notano chiaramente i picchi di precipitazione della ferrite pro-eutettoide e la precipitazione del boruro di ferro. Si nota come il picco corrispondente alla formazione del boruro di ferro sia particolarmente evidente per l'acciaio riscaldato a 1300°C ma sia presente in forma meno intensa anche per temperature di riscaldamento a 1200°C.*



▲  
Fig. 17

$\varphi_2 = 45^\circ$  section of the ODF Euler space as a function of the added micro-alloyed elements and of the final rolling temperature<sup>17)</sup>.

Sezioni ODF a  $\varphi_2 = 45^\circ$  nello spazio di Eulero in funzione dei micro-alliganti aggiunti e della temperatura di fine laminazione<sup>17)</sup>.

crystal grains which permits to well and fully characterize the observed materials. These investigations have allowed to identify with precision the crystallographic textures of the rolled products which are the most suitable to undergo the successive forging operations<sup>30,31,32,33,34,35,36,37)</sup>. In the hot rolled steels the crystallographic textures of the final phases (ferrite, martensite, bainite) depend on the orientations induced in the parent austenite according to precise and well defined relations<sup>38,39,40,41,42,43,44)</sup>. Generally, in the ferrite of the rolled steels the prevailing texture is  $\{001\}[110]$ , where the first term of indexes defines the lattice plane parallel to the rolling plane and the second one indicates the lattice direction parallel to the rolling one. This prevailing component of the textures is generated from  $\{100\}[001]$  (Cube), induced in the recrystallized austenite by the forming process and is not particularly suitable for the successive operations of plastic forming, because the presence of grains featured by  $\{001\}$  plane parallel to the rolling one implies values of  $r_m$  lower than the unity. In the deformed and not recrystallized austenite the texture components  $\{110\}[112]$  (Brass) and  $\{112\}[111]$  (Copper) are formed, generating in the ferritic phase the textures  $\{332\}[113]$  and  $\{113\}[110]$ , respectively. However, the precise association between the texture of the ferrite with a particular texture of the deformed parent austenite cannot be easily stated. Actually, the textures  $\{110\}[001]$  (Goss),  $\{011\}[511]$  (Goss/Brass),  $\{168\}[211]$  (Brass/S),  $\{123\}[634]$  (S),  $\{236\}[322]$  (S/Copper), can produce all the observed and documented transformation textures and also the starting texture can lead to the same final texture. The textures  $\{332\}[113]$ ,  $\{223\}[110]$ ,  $\{112\}[110]$  are the best ones to produce also the cold formed components featured by the complex shapes. In the case of non

deep forging process these textures are very suitable thanks to an average value of  $r_m$  (coefficient of normal anisotropy) higher than 2, while for the deep forming operations the cold rolling and the following annealing treatment are needed to obtain the texture components  $\{111\}[112]$ ,  $\{111\}[110]$  featured by DR (coefficient of planar anisotropy) nearly null<sup>40,41,42,43)</sup>. The development of the texture  $\{332\}[113]$  allows to perform the best combination among formability, strength and toughness. The intensity of this transformation textures can be increased through the addition of Nb, Ti and V, through the high reduction of the thickness and through a strict control of the final rolling temperatures. The presence of other alloying elements such as Mn, Ni, Cr, Mo, a fine size of the austenitic grains and high cooling rates can lead to the development of the most favourable distribution of the crystallographic orientation. On the contrary, the formation of the unfavourable component  $\{113\}[110]$  is not significantly influenced by the former factor of influence. The microalloying with Ti, Nb and V low carbon steels (0.02-0.04%C) is a strategic operation for conditioning the crystallographic texture through a retard produced in the recrystallization process and slowing of the growth rate interesting the recrystallized grains and the ones nucleated after the phase transition from austenite to ferrite.

The introduction of micro-alloying elements allow to use the controlled final rolling temperature to define the final texture of a rolled product which are fundamental to grant the correct formability and anisotropy of a strip (Fig. 17). Variation of few tens of degrees in the final temperature of hot rolling can imply a significant difference on the induced crystallographic texture. It is worth noting that the



control of the induced crystallographic texture can allow a good control design in presence of micro-alloyed elements especially in presence of a simultaneous presence of Nb and V, because the first one control the recrystallization of austenite at high temperature and the second one control the grain formation and the related texture at the austenite-ferrite transition temperature.

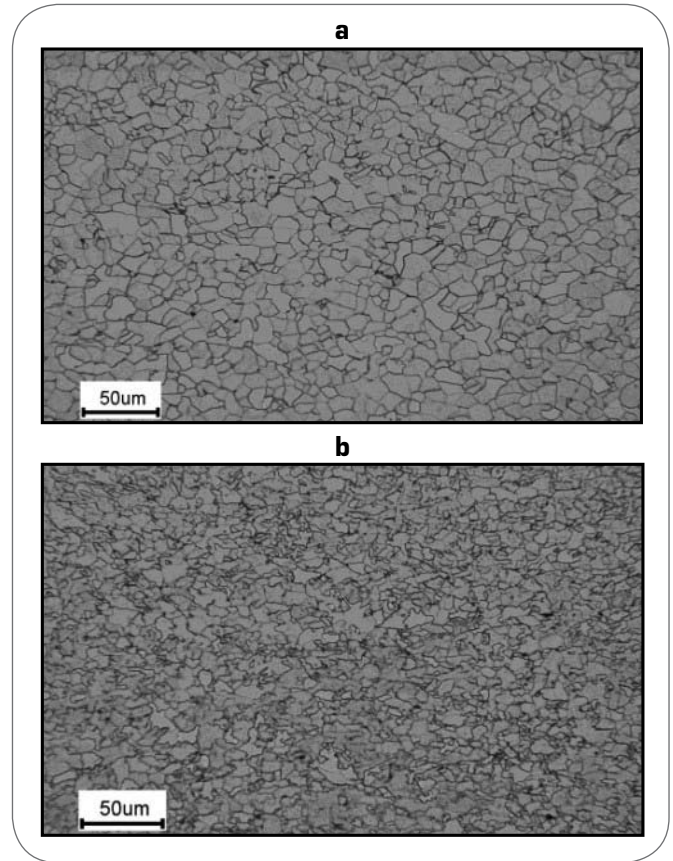
The refinement grain effect can be clearly estimated by the comparison of mild steel and of Nb-V micro-alloyed steel which have followed the same reduction route and have undergone the same final coiling temperature (Fig. 18).

## CONCLUSIONS

The micro-alloying of steels can offer very good opportunity of economic savings associated with high resistance. On the other hand, the correct application of micro-alloying needs the reliable designing of the whole technological route in order to avoid drawbacks related to hot shortness cracks, drop of toughness properties, induction of detrimental crystallographic textures.

## REFERENCES

- [1] T. Gladman, The Physical Metallurgy of Microalloyed Steels, The Institute of Materials, London, 1997, 263-355
- [2] W. Nicodemi, Metallurgia-Principi Generali, Bologna, Zanichelli (2000), 64-66.
- [3] T. Gladman, The Physical Metallurgy of Microalloyed Steels, The Institute of Materials, London, 1997, 81-185.
- [4] C. Mapelli, S. Baragiola, L. Bisaccia, R. Venturini, Rev. Met. Paris, 11 (2003), 1067-1076.
- [5] H. Adrian, A thermodynamic analysis of microalloy precipitation, Proc. of International Symposium "Microalloyed Vanadium Steels", Ass. Polish Met. Eng. And Strator, (1990), 105-124.
- [6] X. M. Wang, X. L. He, ISIJ Int, 42, 2002, Supplement S-8-S46.
- [7] T. Senuma, Physical metallurgy of modern high strength steel sheets, ISIJ International, 41 (2001) 520-532.
- [8] R. Kuziak, T. Bold, Y.W. Cheng, Microstructure control of ferrite-pearlite high strength low alloy steels utilizing microalloying additions, Journal of Materials Processing Technology 53 (1995) 255-262.
- [9] E. El Kashif, K. Asakura, K. Shibata, ISIJ Int., 43 (2003), 2007-2014.
- [10] C. Liu, T. Nagoya, K. Abiko and H. Kimura: Metall. Trans., 23 (1992), 263.
- [11] J.K. Patel, B. Wilshire, The challenge to produce consistent mechanical properties in Nb-HSLA strip steels, Journal of Material Processing Technology, 120 (2002) 316-321.
- [12] A. Bakalloglu, Effect of processing parameters on the microstructure and properties of an Nb microalloyed steel, Materials Letter 56 (2002) 263-272.
- [13] T. Siwecki, B. Hutchinson, S. Zajac, Microalloying 95, Proc. Int. Conf. on Microalloying, Pittsburg, PA, 1995, p. 197.
- [14] V. Ollilainen, W. Kasprzak, L. Holappa, The effect of silicon, vanadium, and nitrogen on the microstructure and hardness of air cooled medium carbon low alloy steels, Journal of Material Processing Technology, 134 (2003) 405-412.



▲  
Fig. 18

**Comparison between the grain size obtained on a (a) mild steel and on a (b) Nb-V micro-alloyed steel which have followed the same reduction route and have undergone the same final coiling temperature<sup>17)</sup>.**

*Confronto tra le dimensioni del grano ferritico in (a) un acciaio non microlegato e (b) in un acciaio microallegato con Nb e V a seguito dell'applicazione dei medesimi passi di riduzione e dopo l'applicazione della medesima temperatura di avvolgimento<sup>17)</sup>.*

- [15] T. Siwecki, A. Sandberg, W. Roberts, R. Lagneborg, Thermomechanical process of microalloyed austenite, in: Ratz A.J., Ratz G.A., Wray P.J. (Eds.), Conf. Proc. TMS-AIME, Warrendale, USA, 1982, p. 163.
- [16] N. Maruyama, R. Uemori, M. Sugiyama, The role of niobium in the retardation of the early stage of austenite recovery in hot-deformed steels, Material Science and Engineering A250 (1998) 2-7.
- [17] R. Riva, C. Mapelli, W. Nicodemi, ISIJ Int., Vol. 47 (2007) No. 8, pp. 1204-1213.
- [18] B. Mintz, ISIJ Int., Vol. 39 (1999) No. 9, pp. 833-855.
- [19] B. Mintz, S. Yue and J. J. Jonas: Int. Mater. Rev., 36 (1991), No. 5, 187.
- [20] J.G. Williams, C.R. Killmore, Barrett J.F., Church A.K., Processing, Microstructure and Properties of HSLA Steels. In: A.J. De Ardo editor, Pittsburg, USA. TMS, 1988, p. 133.
- [21] T. Gladman, R.F. Dewsnap, In. Proc. Conf. on Steels for line pipe and pipeline fittings, Oct. 1981, London. The Metals Soc, 1983, p. 61.
- [22] I. Kozasu, C. Ouchi, I. Sampei, T. Okita, Microalloying '75. New York. Union Carbide; 1977, p. 120.

- [23] A.M.Sage, In: Proc. Conf. on Steels for line pipe and pipeline fittings, Oct 1981, London. The Metals Soc., 1983, p. 39.
- [24] F. J. Humphreys, M. Hatherly, Recrystallization and related annealing phenomena, 2nd edition, Elsevier, 2004, 333-411.
- [25] C. Mapelli, R. Venturini, Flow, Thermal and Microstructural Analysis during Cast Rolling of Steel in In-line Strip Production Process, Steel research 75 (2004) No. 4, 257-265.
- [26] G. Arvedi, L. Manini, A. Bianchi, A. Guindani, F. Mazzolari, U. Siegers, Stahl und Eisen, 17, 3, (2003), 57-69.
- [27] R. K. Ray, J.J. Jonas, M.P. Butrón-Guillén, J. Savoie, ISIJ Int., 34 (1994), 12, 927-942.
- [28] M. P. Butrón-Guillén, J. J. Jonas and R. K. Ray, Acta Metall. Mater., 42 (1994), 3615.
- [29] T. Nakamura, K. Esaka, Proc. of the Int. Conf. on Physical Metallurgy of thermomechanical Processing of Steels and Other Metals, Vol. 2, ISIJ, Tokyo (1988), 644.
- [30] H. Inagaki, Z. Metallkde., 81 (1990), 474.
- [31] M. P. Butrón-Guillén, J. J. Jonas and R. K. Ray, Acta Metall. Mater., 42 (1994), 3615.
- [32] T. Nakamura, K. Esaka, Proc. of the Int. Conf. on Physical Metallurgy of thermomechanical Processing of Steels and Other Metals, Vol. 2, ISIJ, Tokyo (1988), 644.
- [33] H. Inagaki, Z. Metallkde., 81 (1990), 474.
- [34] H. Inagaki, Z. Metallkde., 82 (1991), 26.
- [35] J. R. Hirsch, W. B. Hutchinson and K. Lücke, Texture Microstructure, 14 (1991), 691.
- [36] B. Jonsson, Z. Metallkde., 83 (1992), 349.
- [37] Ph. Chapellier, R. K. Ray, J. J. Jonas, Acta Metall. Mater., 38 (1990), 1475.
- [38] Y. Yutori and R. Ogawa, Proc. 6th Int. Conf. on Textures of Materials, Vol. 1, ISIJ, Tokyo (1981), 669.
- [39] H. Inagaki, Proc. 6th Int. Conf. on Textures of Materials, Vol. 1, ISIJ, Tokyo (1981), 149.
- [40] H. Inagaki, Trans Iron Steel Inst. Jpn., 17 (1977), 166.
- [41] H. Inagaki, Proc. 5th Int. Conf. on Textures of Materials, Vol. 2, Springer Verlag, Berlin (1978), 157.
- [42] G. J. Davies, J. S. Kallend and P. P. Morris, The Hot Deformation of Austenite, AIME, New York (1977), 599.
- [43] H. Inagaki, Z. Metallkde., 74 (1983), 716.
- [44] R. K. Ray, M. P. Butrón-Guillén, J. J. Jonas and G. E. Ruddle, ISIJ Int., 32 (1992), 2, 203-212.

## ABSTRACT

### TEORIA INTRODUTTIVA SULLA MICROALLIGAZIONE

*Parole chiave: acciaio, proprietà*

La microalligazione degli acciai può costituire un'ottima occasione di risparmio, dati i piccoli tenori di elementi microalliganti, che devono essere aggiunti per ottenere il desiderato incremento delle proprietà resistenziali e di tenacità. I microalliganti tradizionalmente aggiunti sono Ti, Nb, V, Al e B. Il boro viene aggiunto per aumentare la tendenza alla formazione della bainite (Figura 5, Figura 6, Figura 7). Al contrario, gli altri elementi alliganti vengono aggiunti al fine di promuovere la precipitazione di particelle di carbo-nitruro (Figura 1) in grado di rafforzare le leghe metalliche attraverso il bloccaggio delle dislocazioni (Figura 2, Figura 3) e l'affinamento del grano ferritico (Figura 4, Figura 18). L'ostacolo offerto dai precipitati incoerenti che non si lasciano attraversare dal movimento delle dislocazioni produce un innalzamento del carico di snervamento, mentre l'affinamento del grano produce sia un incremento del carico di snervamento sia un innalzamento della tenacità. Attraverso l'applicazione di relazioni termodinamiche di equilibrio (1,2,3,4,5,6,7,8,9,10,11,12) è possibile stimare la composizione chimica di carbo-nitruri di composizione complessa, mentre la dimensione dei nano-precipitati formati dai microalliganti è determinata dalla velocità di raffreddamento a cui l'acciaio viene sottoposto. Le condizioni di precipitazione migliore, che prevedono un'elevata frazione in volume di nano-precipitati ma un irrisorio accrescimento degli stessi si può realizzare attraverso rapidi raffreddamenti (Figura 9, Figura 10), poiché tale condizione consente una fine dispersione dei nano-precipitati. Per quanto concerne gli acciai microalligati al boro bisogna porre attenzione affinché il riscaldamento precedente il raffreddamento -volto a indurre i costituenti strutturali desiderati (bainite e

ferrite aciculare)- consenta un significativo accumulo di boro in soluzione sul bordo dei grani (Figura 13) senza però consentire la formazione di boruro di ferro (Figura 16). Nel caso dei micro-alliganti formanti i precipitati ceramici uno dei maggiori problemi di danneggiamento è legato all'abbassamento di duttilità a caldo conseguente alla precipitazione dei carbo-nitruri in corrispondenza del bordo grano (Figura 14, Figura 15); un altro inconveniente da evitare è l'eccessivo ingrossamento dei precipitati, eventualmente caratterizzati da forme spigolose e quindi da un elevato fattore di intensificazione degli sforzi, che possono divenire anche l'elemento nucleante delle cricche di fatica (Figura 12). In quest'ultimo caso gli acciai micro-alligati con titanio devono essere trattati con estrema cura, al fine di evitare la formazione di precipitati ceramici di dimensione eccessivamente elevata.

I precipitati ceramici formati dai microalliganti risultano particolarmente efficaci anche nel controllo dello sviluppo delle tessiture cristallografiche in forza della loro interazione sia con i bordi dei grani austenitici sia dei bordi ferritici, poiché ne alterano le dinamiche di ricristallizzazione ed accrescimento. In particolare, combinazioni a base di Nb e V risultano particolarmente efficienti, poiché i precipitati del niobio interagiscono con i grani austenitici, in virtù dell'alta temperatura di precipitazione, mentre i precipitati del vanadio controllano la nucleazione e l'accrescimento delle strutture ferritiche, che si formano nel medesimo intervallo di temperatura di precipitazione dei carbo-nitruri di vanadio (Figura 17).

L'applicazione della micro-alligazione non si può ridurre alla semplice formulazione di particolari composizione chimiche, ma necessita di una corretta progettazione dell'intero ciclo produttivo volto ad ottimizzare l'effetto dei micro-alliganti e ad evitare l'insorgere di fenomeni nocivi che possono compromettere significativamente la tenacità, la duttilità a caldo o promuovere l'insorgere di cricche di fatica.